

Review

Feasibility of Preparing Steel Slag–Ground Granulated Blast Furnace Slag Cementitious Materials: Synergistic Hydration, Fresh, and Hardened Properties

Jianwei Sun ^{1,2,*}, Shaoyun Hou ^{1,2}, Yuehao Guo ^{1,2}, Xinying Cao ^{1,2} and Dongdong Zhang ³

¹ School of Civil Engineering, Qingdao University of Technology, Qingdao 266520, China; houshaoyun19980120@163.com (S.H.); kiki2438199144@163.com (Y.G.); lc211008@126.com (X.C.)

² Engineering Research Center of Concrete Technology under Marine Environment, Ministry of Education, Qingdao 266520, China

³ Jinan Rail Transit Group Co., Ltd., Jinan 250000, China; 15628861197@163.com

* Correspondence: jianwei_68@126.com

Abstract: Steel slag and GBFS are wastes generated during the steel and iron smelting process, characterized by their considerable production rates and extensive storage capacities. After grinding, they are often used as supplementary cementitious materials. However, the intrinsic slow hydration kinetics of steel slag–GBFS cementitious material (SGM) when exposed to a pure water environment result in prolonged setting times and diminished early-age strength development. The incorporation of modifiers such as gypsum, clinker, or alkaline activators can effectively improve the various properties of SGM. This comprehensive review delves into existing research on the utilization of SGM, examining their hydration mechanisms, workability, setting time, mechanical strengths, durability, and shrinkage. Critical parameters including the performance of base materials (water-to-cement ratio, fineness, and composition) and modifiers (type, alkali content, and dosage) are scrutinized to understand their effects on the final properties of the cementitious materials. The improvement mechanisms of various modifiers on properties are discussed. This promotes resource utilization of industrial solid wastes and provides theoretical support for the engineering application of SGM.

Keywords: steel slag; GBFS; hydration; mechanical property; durability; shrinkage



Citation: Sun, J.; Hou, S.; Guo, Y.; Cao, X.; Zhang, D. Feasibility of Preparing Steel Slag–Ground Granulated Blast Furnace Slag Cementitious Materials: Synergistic Hydration, Fresh, and Hardened Properties. *Buildings* **2024**, *14*, 614. <https://doi.org/10.3390/buildings14030614>

Academic Editor: Mizan Ahmed

Received: 5 January 2024

Revised: 5 February 2024

Accepted: 7 February 2024

Published: 26 February 2024



Copyright: © 2024 by the authors. Licensee MDPI, Basel, Switzerland. This article is an open access article distributed under the terms and conditions of the Creative Commons Attribution (CC BY) license (<https://creativecommons.org/licenses/by/4.0/>).

1. Introduction

Steel slag, a nonmetallic by-product generated during the steelmaking process, accounts for approximately 15–20% of crude steel production [1–3]. Globally, steel slag production is estimated to be around 190–280 million tons per year, with China contributing approximately 50% of the total and its production continuing to rise [4–6]. With proper utilization, steel slag can not only contribute to resource conservation but also reduce environmental pollution. Additionally, the comprehensive utilization of steel slag has the potential to lower production costs and enhance economic benefits. The utilization of steel slag in Japan, Europe, the United States, and China is shown in Figure 1. Steel slag can be disposed of in road engineering, cement production, internal recycling, civil engineering, and agriculture in Japan, Europe, the United States, and China [2–6]. It is noteworthy that 30–50% of steel slag is used for road construction in other countries, while more than 70% of steel slag is for final disposal. Therefore, compared to developed countries such as the United States and Japan, which achieve nearly 100% utilization rates, the actual comprehensive utilization rate of steel slag in China is only 30% [2,3]. The low utilization rate of steel slag results in a significant accumulation of waste, occupying land resources and posing environmental risks because of the leaching toxicity of heavy metals like Mn and Cr. This situation impedes the sustainable development of the steel industry [7–9]. Consequently, it has become crucial to address how to increase the comprehensive utilization rate of steel slag and transform it from waste into a valuable resource.

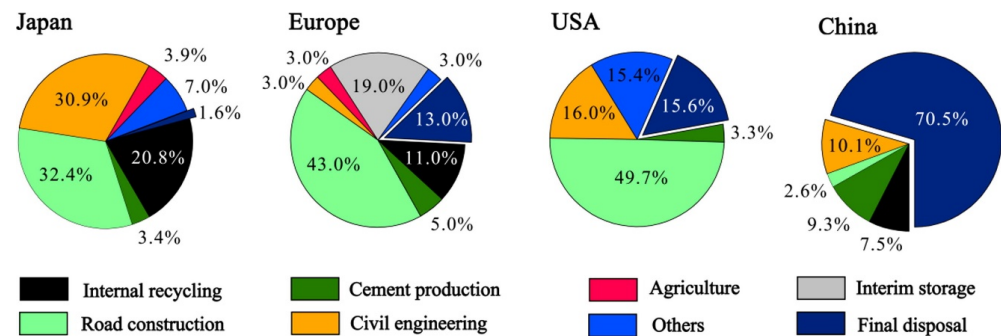


Figure 1. Steel slag utilization in Japan, Europe, the United States, and China [2].

The predominant form of steel slag in China is derived from the converter process, composing approximately 70% of the accumulated steel slag reserves. Steel slag contains a large amount of inactive components, mainly composed of the RO phase (MgO-FeO-MnO solid solution) [7–13]. Its active components, including tricalcium silicate (C_3S), dicalcium silicate (C_2S), calcium aluminate, and calcium iron aluminate, are similar to the active components of Portland cement clinker [7–13]. Owing to these similarities, steel slag exhibits a measure of hydraulicity, which has led to its designation as a ‘substandard cement’ or low-quality cement. This identifies it as a prospective sustainable cementitious material with inherent green qualities. However, because of the limited number of active phases in steel slag, when it is used solely as a cementitious material, it has inherent drawbacks such as a slow reaction rate, low degree of reaction, and slow development of early strength [14,15]. Given the shared metallurgical lineage between steel slag and ground granulated blast furnace slag (GBFS), the former is being considered for cotreatment with the latter to improve its performance as a cementitious material. The main phase of GBFS is amorphous and has high reactivity. When steel slag is mixed with GBFS, the clinker-like characteristics of steel slag and the pozzolanic reaction characteristics of GBFS can mutually promote the hydration process, significantly improving the hydration degree of the composite system, especially the later strength of the composite material. However, the application of steel slag–GBFS cementitious material (SGM) remains limited due to extended setting times and inadequate early strength, which fail to satisfy the demands of various engineering requirements [16–28]. A bibliometric study based on the Web of Science database is finished and shown in Figure 2. As can be seen, there has been an increasing amount of research on SGM in the past 15 years. In particular, after 2020, the number of published papers doubled compared to before. This indicates that scholars are increasingly valuing the development of SGM and have high expectations for this low-carbon material. To remedy these deficiencies of SGM, modifiers such as gypsum, cement clinker, and alkaline activators are applied. From statistical data, it can be seen that with the development of alkali-activated cementitious materials, over 50% of studies have used alkaline activators as effective modifiers of SGM. The proportion of research on various types of gypsum as modifiers is 21.05%. However, the research on cement clinker as a modifier is only 9.47%. Using modifiers accelerates the development and application of SGM in the field of cementitious materials. From the perspective of green development and solid waste utilization, further research on using by-product gypsum as a modifier is needed.

Based on extensive research by both domestic and international scholars on SGM, this paper analyzes and summarizes the existing research results from the perspectives of hydration characteristics, setting time, and workability of fresh mortar, mechanical properties, durability, and volume shrinkage of hardened mortar. Furthermore, the paper delves into the effects of modifiers on the performance of SGM. It elucidates how these materials improve the overall characteristics of cementitious materials while also providing an in-depth analysis of the underlying mechanisms that contribute to this enhancement. Finally, the existing issues in current research and future development trends are analyzed

and discussed, aiming to provide theoretical support for the application and promotion of SGM.

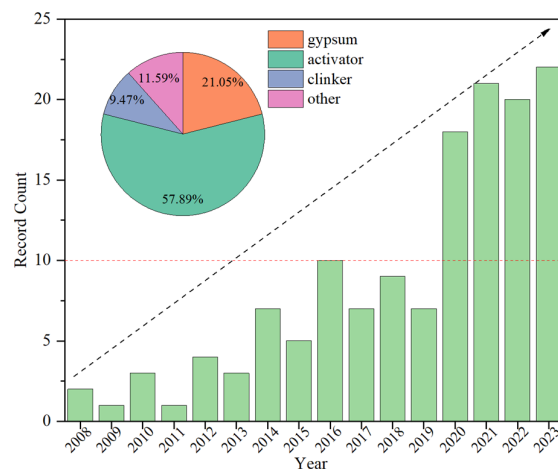


Figure 2. Record count in the field of SGM.

2. Synergistic Hydration of SGM

Steel slag itself exhibits a certain degree of hydraulicity and can react with water at room temperature, while GBFS has limited reactivity with water and requires activation in an alkaline environment with a pH value higher than 12.5 [29–32]. Studies have found that when steel slag and GBFS are mixed, there is a synergistic effect in terms of hydration [33,34]. The hydration mechanism of SGM is illustrated in Figure 3. Upon contact with water, active components such as calcium aluminate and C_3S in steel slag dissolve, releasing Ca^{2+} , OH^- , and small amounts of Al^{3+} and Si^{4+} . This results in an increase in the pH of the pore solution, represented by the “steep and high” first exothermic peak (S1) in the heat evolution rate curve [34]. After a short induction period (S2), the early hydration of the small amount of calcium aluminate, C_3S , and β - C_2S in steel slag leads to the acceleration of hydration and the formation of the second peak (S3) [34]. At this stage, Si-O-Al and Si-O-Si bonds in the GBFS are broken in the alkaline environment [34]. The hydration products of steel slag, namely $Ca(OH)_2$ and C-S-H gel, precipitate and cover the surfaces of C_3S and C_2S particles, thereby reducing the hydration rate and entering the deceleration period (S4) [34]. After a long stabilization period (S5), the hydration of Si-O-Al and Si-O-Si bonds in the GBFS, along with the reaction between $[SiO_4]^{4-}$ and $[AlO_4]^{5-}$ released from GBFS and $Ca(OH)_2$ in the system, lead to the reacceleration of the reaction rate and the appearance of the third exothermic peak (S6) [34]. As hydration progresses, two types of gel products, namely calcium silicate hydrate (C-S-H) gel and calcium aluminate hydrate (C-A-H) gel, accumulate on the surfaces of mineral particles, and the rate of volcanic ash reaction gradually decreases and tends to stabilize (S7) [34–40]. Some researchers have suggested that the highest reaction degree is achieved when the mass ratio of steel slag to GBFS is 1:1 or 2:3 [16–20]. It is important to note that the products of volcanic ash reaction are not solely C-S-H and C-A-H gels but also include calcium aluminosilicate hydrate (C-A-S-H) gel.

Due to the limited alkalinity provided by the self-hydration of steel slag, SGM is known to have slow reaction rates and a lack of early strength. In order to address this issue, SGM is commonly modified with materials such as gypsum (natural gypsum and industrial by-product gypsum), cement clinker, or alkaline activators (e.g., sodium silicate, $Ca(OH)_2$, NaOH, and Na_2CO_3) [41–49]. $Ca(OH)_2$, formed by the hydration of cement clinker and OH^- provided directly by alkaline activators, creates a more alkaline environment for cementitious materials, promoting the dissociation of $[SiO_4]^{4-}$ and $[AlO_4]^{5-}$ in the GBFS and further improving the early strength of materials. However, excessive amounts of certain modifiers, such as excessive cement clinker, NaOH, and Na_2CO_3 , may actually reduce the later strength of materials. This is because in the later stages of hy-

dration, excessive OH^- or CO_3^{2-} combine with Ca^{2+} on the surface of particles to form excessive $\text{Ca}(\text{OH})_2$ and CaCO_3 , hindering continuous hydration of both steel slag and GBFS particles [42]. On the other hand, sodium silicate plays a dual activation role by providing OH^- and $[\text{SiO}_4]^{4-}$, thereby not only offering an alkaline environment but also supplying the necessary silicon source for reactions, ensuring the development of later strength [50–52].

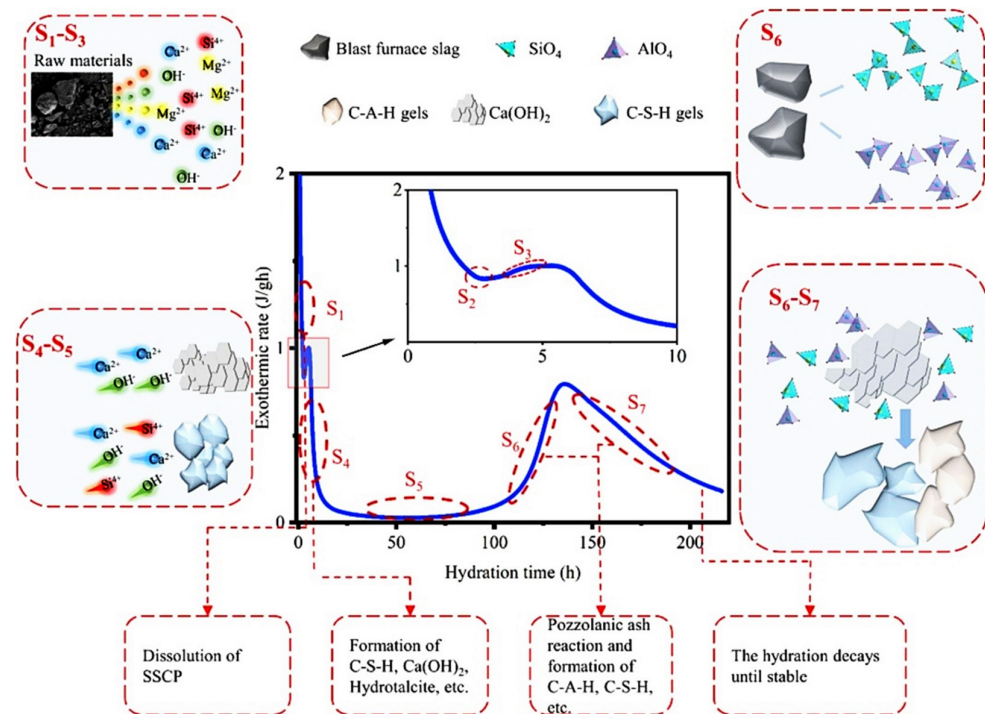


Figure 3. Hydration mechanism of SGM [34].

Gypsum is an effective modifier, and steel SGM with gypsum system exhibits excellent performance. Studies have shown that steel slag, GBFS, and gypsum exhibit significant synergistic effects during the hydration process [53,54]. These effects are mainly attributed to the reactions where the OH^- provided by steel slag, the Al^{3+} from steel slag and GBFS, and the SO_4^{2-} from gypsum react with the Ca^{2+} . This reaction causes the formation of insoluble calcium aluminate (AFt), driving the continuous progress of the reaction [55]. Xu et al. [56] investigated the effects of three types of industrial by-product gypsum, namely desulfurization gypsum (DG), desulfurization ash (DA), and fluorogypsum (FG), on the hydration and hardening properties of SGM. The results indicate that in the early stages, needle-rod-shaped AFt and amorphous gel are formed in all three cementitious systems. However, the DA system, which has a lower gypsum content, shows a significantly lower amount of AFt compared to the other systems. In the later stages, both the DG system and the FG system exhibit similar structures, characterized by interlaced AFt and gel filling and encapsulation. In contrast, the DA system only shows gel formation without a distinct AFt structure. As a result, the presence of AFt in the DG and FG systems contributed to the higher early strength of SGM. The microstructures of the hardened pastes in the DG and DA systems are shown in Figure 4. The gel morphology differs significantly between the two systems. The gel in the DG system appears cluster-like (Figure 4a), while the gel in the DA system exhibits a network-like structure due to the relatively higher amount of space provided by the lower AFt content (Figure 4b). The hydration mechanism of these three composite systems using the DG system as an example is shown in Figure 5. In the initial stages, the hydration of steel slag (Equation (1)) and the dissolution of DG release OH^- , Ca^{2+} , and SO_4^{2-} . At the same time, under alkaline conditions, Si-O-Al and Si-O-Si bonds in the GBFS are broken, resulting in the formation of $[\text{SiO}_4]^{4-}$ and $[\text{AlO}_4]^{5-}$

monomers. Subsequently, the reaction between Ca^{2+} , SO_4^{2-} , and $[\text{AlO}_4]^{5-}$ produces AFt (Equation (2)), while the reaction between Ca^{2+} and $[\text{SiO}_4]^{4-}$ leads to the formation of C-S-H gel (Equation (3)). Finally, the continuous production of C-S-H gel fills and encapsulates the interwoven AFt, ensuring the development of later strength. Therefore, the ultimate products of SGM with gypsum are C-S-H gel and AFt [56].

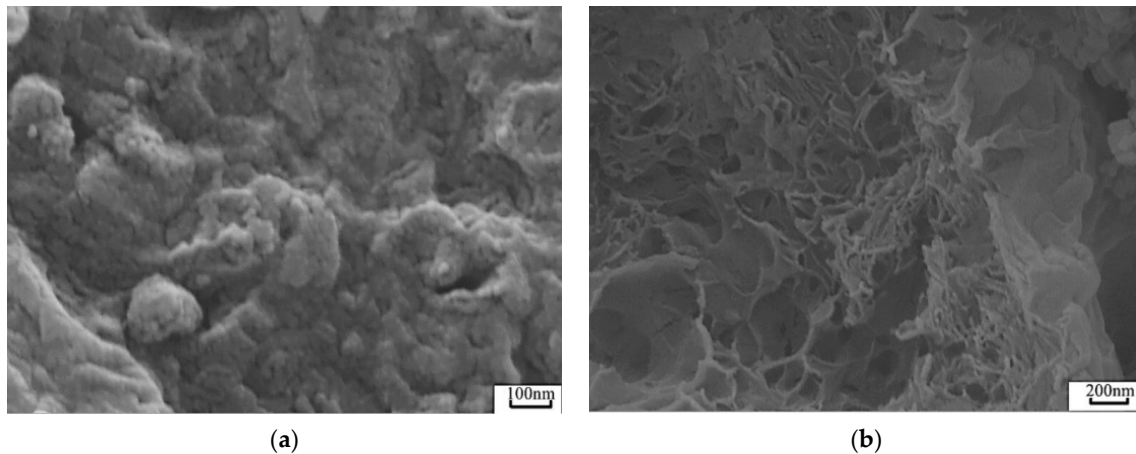
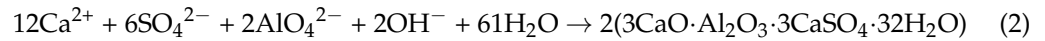
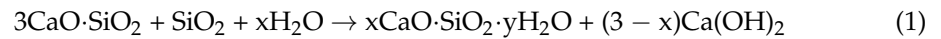


Figure 4. Microstructures of steel slag–GBFS–IBG hardened pastes: (a) gel in DG; (b) gel in DA [56].

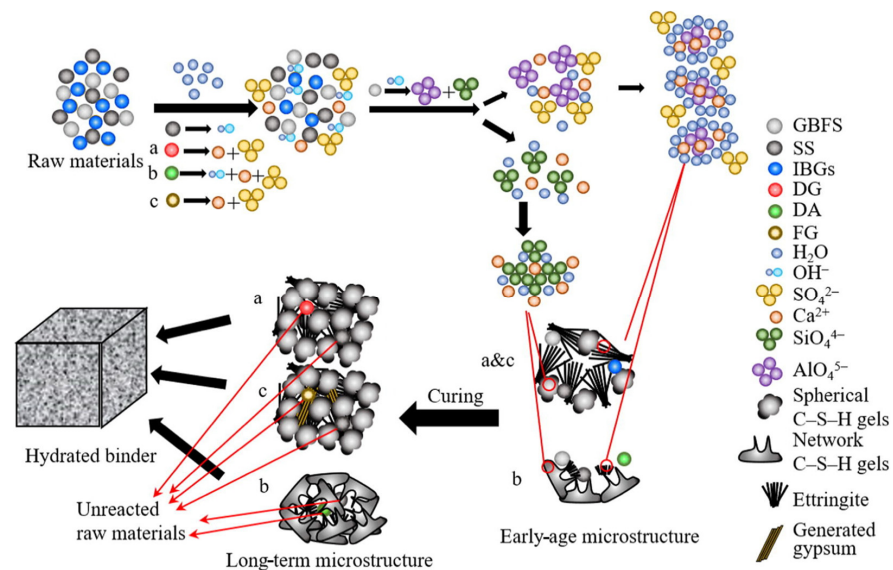


Figure 5. Hydration mechanism of steel slag–GBFS–IBG cementitious material [56].

When cement clinker is used as a modifier, its effectiveness is limited. Zhao et al. [57] prepared various SGMs and compared them with the Portland cement system to study the differences in hydration processes and pore structures. Overall, the cumulative heat of SGM at all ages is lower than that of Portland cement, and the cumulative heat within 72 h is less than 50% of that observed in the Portland cement system. This indicates that the alkaline environment provided solely by the hydration of clinker is relatively weak and insufficient to significantly enhance the initial hydration rate and reaction degree of steel slag and GBFS [58]. Regarding the pore structure, the total porosity of hardened SGM pastes is observed to be higher compared to that of hardened Portland cement pastes. Thus,

the ternary system exhibits lower density and significantly lower strength when compared to the Portland cement system. These findings suggest that the use of cement clinker as a modifier in SGM may have limitations in terms of improving the hydration rate and enhancing the mechanical properties of materials. Therefore, alternative modifications such as the addition of gypsum or alkaline activators should be considered to optimize the performance of SGM.

When alkaline activators are used as modifiers, they generally provide a higher alkaline environment than cement clinker, resulting in a higher hydration degree of steel slag and GBFS. You et al. [47] studied the hydration process of alkali-activated SGM and compared the hydration rate and cumulative heat with the Portland cement system (Figure 6). The heat rate and cumulative heat of alkali-activated GBFS materials exhibit similar hydration processes to those of Portland cement. However, alkali-activated SGM has a lower and delayed peak value of the main peak compared to the alkali-activated GBFS material. This is primarily due to the lower reactivity of steel slag, which causes a delay in the appearance and reduces the peak value of the main exothermic peak. The cumulative heat within 7 h of the alkali-activated SGM is higher than that of the Portland cement system, but within 72 h, it was only 53% of that of Portland cement. This indicates that alkali-activated SGM has a higher early-stage heat and functions as a low-heat cementitious material. Furthermore, the incorporation of retarders effectively delays the occurrence of the main exothermic peak and reduces the hydration rate of alkali-activated SGM, prolonging the setting time of materials. In terms of hydration products, C-A-S-H gel is the main product in alkali-activated SGM. The relative content of steel slag and GBFS does not change the type of hydration products but can affect the structure of gel products. With an increase in GBFS content, the Ca/Si ratio in C-A-S-H gel gradually reduces, while the Al/Si ratio increases. In general, Al tetrahedrons are substituted into the paired sites of Si-O tetrahedron chains, and Si or Al tetrahedrons are connected to form a frame structure by sharing one oxygen atom in C-(A)-S-H gels [50]. The composition of C-A-S-H in alkali-activated material relies on the calcium and aluminum contents of precursors [50]. Therefore, the change in ratios is related to the higher aluminum content in GBFS. In relation to pore structure, compared to Portland cement, alkali-activated SGM has a lower total porosity and a higher number of gel pores but fewer capillary pores. This may be due to the higher content of C-A-S-H gel in alkali-activated SGM compared to C-S-H gel in Portland cement [54–60]. Compared to alkali-activated GBFS material, alkali-activated SGM has a higher porosity and fewer gel pores. Similarly, compared to alkali-activated steel slag material, alkali-activated SGM exhibits a reduced content of small pores and a decreasing trend in porosity with the increase in GBFS content, indicating that GBFS plays a role in refining the pore structure [54–60].

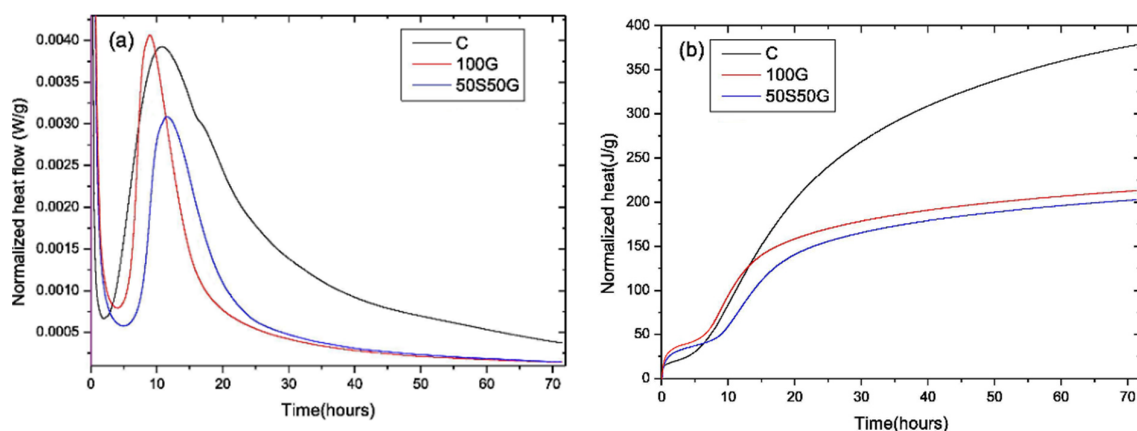


Figure 6. Hydration heat evolution curves of alkali-activated cementitious material and Portland cement: (a) exothermic rate; (b) cumulative hydration heat. (C: cement; 100G: 100% GBFS; 50S50G: GBFS: steel slag = 1:1) [47].

3. Fresh Properties of SGM

3.1. Fluidity

There is limited research specifically focusing on the fluidity of binary systems of SGM, as well as ternary systems of SGM containing gypsum. However, there are studies regarding the fluidity of SGM modified with alkaline activators. It has been found that when sodium silicate is used as the activator, the flowability of SGM with a mass ratio (steel slag/GBFS) of 1:1 and 0:1 is reported to be 230 mm and 270 mm, respectively. The specific surface areas of steel slag and GBFS used in these systems are recorded as 370 m²/kg and 436 m²/kg [49]. For alkali-activated SGM with mass ratios of 8:2, 9:1, and 10:0 and specific surface areas of 458 m²/kg and 430 m²/kg for steel slag and GBFS, the flowability is measured as 257 mm, 249 mm, and 234 mm, respectively [59]. Generally, under the same alkaline environment and normal curing conditions, the fluidity of alkali-activated SGM is better than that of alkali-activated GBFS binder and alkali-activated steel slag binder. This is due to the higher reactivity of GBFS compared to SGM in the same alkaline environment. It is also noted to be slightly better than that of Portland cement.

3.2. Setting Time

The reaction of SGM is typically slow, leading to a relatively long setting time of the paste. Tsai et al. [51] observed that the relative content of steel slag and GBFS has a significant impact on the setting time of SGM in systems. Under standard curing conditions, when the mass ratio of steel slag to GBFS is 1:9, the setting time can reach 4 d. On the other hand, when the ratio is below 7:3, the setting time is reduced to only 0.5 h. This indicates that as the steel slag content increases, the setting time of SGM reduces. This observation can be attributed to the fact that higher steel slag content more effectively promotes the pozzolanic reaction of GBFS.

In the system of SGM with cement clinker, the research finished by Zhao et al. [57] shows that under standard curing conditions, when the relative content of steel slag, GBFS, and cement clinker is 35:35:30 and the water-to-binder ratio is 0.35 the initial and final setting times of SGM (sample RBC) are 250 min and 325 min, respectively. These setting times significantly exceed those of Portland cement (sample PC). Additionally, when the raw materials meet the Fuller particle distribution (samples F-1#–F-5#), the initial and final setting times are significantly reduced but still remain longer than the setting time of Portland cement (Figure 7).

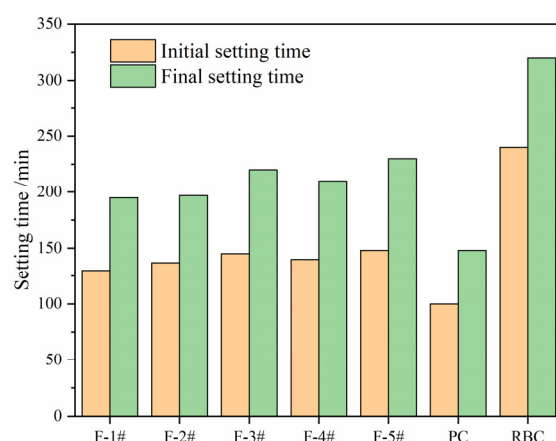


Figure 7. Setting times of pastes [57].

When alkaline activators are used as modifiers in SGM, the setting time is further reduced compared to cement-modified binder systems. This is due to the higher alkaline environment provided by the alkaline activators. You et al. [47] found that the setting time of water glass-activated SGM is only 50 min, which is much shorter than that of cement. Moreover, with the increase in steel slag content in SGM, there is a slight prolongation of

the initial setting time. Some scholars believe that this can be due to the lower solubility of steel slag compared to GBFS [61–64]. The presence of a large number of inert components, primarily in the form of the RO phase in steel slag, reduces the content of active components. These inert components also do not dissolve in an alkaline environment [61–68].

It is important to note that while alkaline activators can significantly reduce the setting time of SGM compared to cement-modified systems, the setting time may vary depending on the composition and properties of the SGM mixture. Further research is needed to investigate and optimize the setting time of SGM in different formulations to meet specific application requirements.

4. Hardened Properties of SGM

4.1. Mechanical Strength

In the binary composite system of SGM, the early reaction rate of steel slag and GBFS is extremely slow, leading to a severe lack of early strength. However, when modified with gypsum, SGM exhibits improved early and later strength. With a mass ratio of 2:7 for steel slag and GBFS, gypsum content of 12%, and a sand ratio of 0.42, the 1 d compressive strength of concrete cured at 45 °C can reach 24.06 MPa, and the 28 d compressive strength can reach 51.54 MPa [68]. The strength of SGM is influenced by the relative content of each component. Cui et al. [17] conducted a study on the influence of steel slag content on the compressive strength of SGM at 3 d, 7 d, and 28 d under standard curing conditions, as depicted in Figure 8. The results show that increasing the relative content of steel slag has little effect on the compressive strength at 7 d and 28 d, but it gradually reduces the compressive strength at 3 d, and the decrease becomes more significant when the steel slag content exceeds 30%. This is because in the early hydration stage, the insufficient filling effect of steel slag as a micro-aggregate cannot compensate for its low reactivity, and with a higher content of steel slag, the low content of GBFS cannot provide enough amorphous active components such as aluminosilicate, which affects the hydration synergy among steel slag, GBFS, and gypsum. Other scholars focus on the influence of GBFS content on the strength of SGM. Zhang et al. [63] found that under standard curing conditions, the compressive strength at different periods is the highest when the relative content of steel slag, GBFS, and gypsum is 29:58:13. However, as the GBFS content increases, the decrease in later strength becomes more pronounced. In addition, the dosage of gypsum, as an important modifier, also has limitations. Xu et al. [69] discovered that raising the curing temperature appropriately helps improve the mechanical properties of the binder at all ages. The higher the temperature, the higher the optimal relative content of steel slag. Under the same mix proportion, the 1 d and 28 d compressive strength of concrete with a mass ratio of steel slag to GBFS of 0.55, gypsum content of 15%, and a sand ratio of 0.43 cured at 45 °C are 27.23 MPa and 49 MPa, respectively. These are significantly higher than the 1 d and 28 d compressive strength of concrete cured at 20 °C, with an increase of approximately 22.15 MPa and 7 MPa, respectively [69]. This is because the higher temperature facilitates the dissolution and deflocculation of active components in steel slag and GBFS [70–74].

When a small amount of cement clinker is used as a modifier, the later compressive strength of SGM is comparable to that of the Portland cement system, but its early strength benefits from the disaggregation of the glassy phase in GBFS and the dissolution of active components in steel slag, thereby improving the strength at all ages. However, the higher content of clinker has a negative effect on the hydration of SGM [49]. Li et al. [48] found that $\text{Ca}(\text{OH})_2$ formed by the hydration of cement increases the alkalinity of the liquid phase. However, if the content of cement is too high, it can actually decrease the strength of the system. This is because when there is an excess amount of cement, the concentration of Ca^{2+} in the early solution quickly reaches saturation, making it difficult for it to react with GBFS in a timely manner, impeding the dissolution of calcium aluminate and calcium silicate in steel slag [75–77].

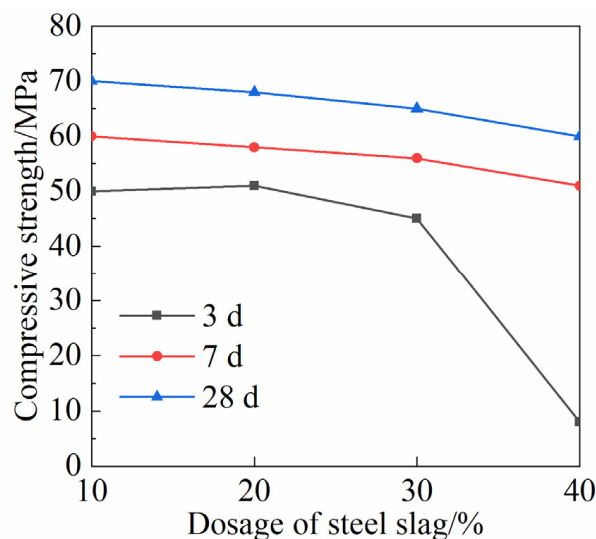


Figure 8. Influence of steel slag content on compressive strength of SGM with gypsum system [17].

Providing an alkaline environment directly is the easiest way to improve the mechanical properties. Research has shown that several commonly used alkaline activators have different stimulating effects on SGM, with water glass having the best effect, followed by NaOH, Na₂SO₄, and Na₂CO₃ having the worst effect [34,77]. When water glass is used as the alkaline activator, the 28 d compressive strength can reach 76.6 MPa thanks to the dual stimulation of OH⁻ and [SiO₄]⁴⁻. However, when the water glass content is too high, the strength actually decreases. This is because the rapidly generated hydration products cannot diffuse in time and adhere to the surface of steel slag and GBFS particles, hindering further hydration [57]. In contrast to the results of cement modification, when water glass is used as an activator, the compressive strength of SGM at different ages can be comparable to or even slightly better than that of Portland cement [57]. In an alkaline environment, increasing the relative content of steel slag will decrease the compressive strength of the system [57,63,78–80]. In experiments conducted by You et al. [47], when water glass is used as an alkaline activator, the 1 d and 28 d compressive strength of alkali-activated GBFS material (sample 100G) under standard conditions are 37 MPa and 72.5 MPa, respectively. After replacing 50% of GBFS with steel slag (sample 50S50G), the compressive strength at 1 d and 28 d decreases by about 28% and 10%, respectively, but still reaches the strength level of the Portland cement system (Figure 9). In addition to the alkaline activators containing Na, some activators containing Ca, such as CaO and Ca(OH)₂, can also have good activation effects. These activators not only provide an alkaline environment but also provide more Ca for hydration. In this case, the effect of the activators is more similar to that of clinker [80,81]. Wang et al. [78] added a small amount of Ca(OH)₂ to the water glass-activated SGM and found that with only a 2% addition of Ca(OH)₂, the compressive strength at 1 d and 28 d reached approximately 57 MPa and 89 MPa, respectively. Compared to the system without Ca(OH)₂, the compressive strength increases by about 27% and 25%, respectively. This is mainly attributed to the large amount of active Ca²⁺ provided by Ca(OH)₂, which promotes the formation of silicate and aluminosilicate networks and provides nucleation sites for C-S-H gel, thus promoting hydration.

In summary, while the early compressive strength is a key performance indicator of SGM and has received much attention, research on mechanical properties such as tensile strength, flexural strength, and elastic modulus is still lacking, and there is still insufficient emphasis on the later strength.

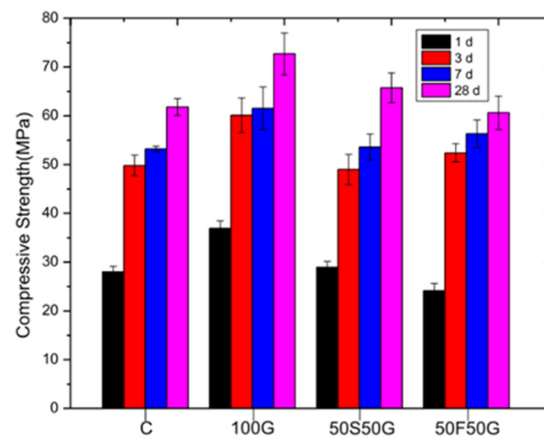


Figure 9. Mechanical properties of alkali-activated material and cement [58].

4.2. Durability

Currently, there is no research specifically focused on the durability of the binary system of SGM, the ternary system of SGM with gypsum, or the ternary system of SGM with cement clinker. However, there have been some studies on the durability of SGM under alkaline conditions.

Regarding water resistance, You et al. [47] compared the water absorption of Portland cement mortars, alkali-activated SGM mortars, and alkali-activated GBFS mortars with the same strength grade, as shown in Figure 10. They found that alkali-activated materials have lower water absorption compared to Portland cement of the same strength grade, and the water absorption of alkali-activated SGM is slightly higher than that of alkali-activated GBFS material, indicating that increasing the steel slag content increases the water absorption, which in turn increases the risk of concrete moisture content, deformation, and cracking.

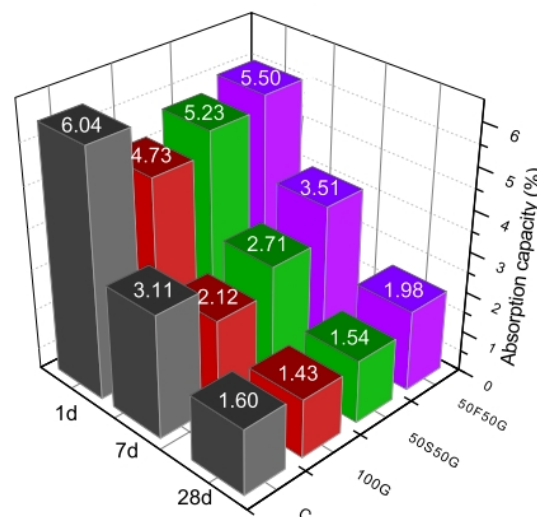


Figure 10. Water absorption capacity of different mortars at the same strength level [47].

In terms of frost resistance, Xiang et al. [76] observed that the average dynamic modulus of elasticity of alkali-activated SGM decreased to 66% of the original value after 300 cycles of freeze–thaw. The mass loss is only 1.1% and the frost resistance reaches the F300 level. Li et al. [77] compared the durability of alkali-activated steel slag material with Portland cement and found that the frost resistance of alkali-activated steel slag cementitious materials was better than that of Portland cement. The compressive strength loss rate and mass loss rate of alkali-activated steel slag cementitious materials after 50 freeze–thaw cycles are 5.9% and 1.03%, respectively, lower than the values of 9.6% and

1.11% for Portland cement. This is due to the low pore volume and high content of gel pore in the hardened paste of alkali-activated SGM, resulting in a denser pore structure with fewer interconnected cracks formed during freeze–thaw cycles [38].

In terms of carbonation resistance, Xiang et al. [76] observed that the carbonation depth of alkali-activated SGM was only 0.3 mm after 28 d under the condition of $20 \pm 3\%$ CO₂ concentration and $70 \pm 5\%$ relative humidity, indicating a negligible level of carbonation.

In terms of resistance to chloride ion penetration, Xiang et al. [76] conducted tests using the electrical flux method and found that the average charge passed within 6 h for alkali-activated SGM was less than 1000 C, indicating very low permeability to chloride ions. You et al. [47] compared the chloride ion resistance of alkali-activated SGM with Portland cement using the rapid chloride migration coefficient method and found that alkali-activated SGM exhibited better resistance to chloride ion penetration, with a chloride ion diffusion coefficient of only one-seventh of that of Portland cement. This is mainly due to the lower interconnected pore volume in alkali-activated SGM compared to Portland cement and the formation of C-A-S-H gel as the main hydration product in alkali-activated SGM, which results in slower chloride ion migration compared to C-S-H gel [78–80].

Overall, compared to Portland cement, SGMs with alkaline activators demonstrate excellent water resistance, frost resistance, carbonation resistance, and resistance to chloride ion penetration. This provides a solid foundation for their design and application in long-life and highly durable materials.

4.3. Shrinkage

Shrinkage may lead to internal tensile stresses and bring a risk of cracking, causing structural instability [80–82]. Currently, there is limited research on the volume stability of SGM, SGM with gypsum, and SGM with clinker. However, there is a scarcity of studies specifically investigating the volume stability of alkali-activated SGM. Research conducted by You et al. [47] indicated that the autogenous and drying shrinkage of alkali-activated SGM falls between those of Portland cement and alkali-activated GBFS cementitious materials (Figure 11). It should be noted that alkali-activated GBFS cementitious materials tend to exhibit high shrinkage, which can be partially mitigated by adding steel slag. However, even with the addition of steel slag, the shrinkage of alkali-activated SGM remains higher than that of cement. In terms of autogenous shrinkage, the autogenous shrinkage of alkali-activated SGM mainly occurs within the first 3 d and is approximately 0.7 times that of alkali-activated GBFS cementitious materials and twice that of Portland cement. Concerning drying shrinkage of alkali-activated SGM, it develops rapidly in the early stages, specifically before 28 d, and then slows down. The drying shrinkage at 28 d is approximately 0.7 times that of alkali-activated GBFS cementitious materials but still much higher than that of Portland cement. This is attributed to the main hydration product of alkali-activated GBFS cementitious materials, C-A-S-H gel, which experiences significant shrinkage under dry conditions [83–85]. The inclusion of low-reactivity steel slag in the system acts as a micro-aggregate, partially inhibiting the drying shrinkage of alkali-activated SGM [86]. Research by Sun et al. [50] also demonstrated that the drying shrinkage of alkali-activated steel slag cementitious materials decreases with increasing content of steel slag. For instance, when steel slag content reaches 30%, the 180 d drying shrinkage value is 3070×10^{-6} , but when the steel slag content is 70%, the 180 d drying shrinkage value drops to only 490×10^{-6} , reducing by approximately six times. This suggests that increasing the steel slag content significantly improves the drying shrinkage of alkali-activated steel slag cementitious materials.

Overall, the shrinkage of alkali-activated steel slag cementitious materials is still higher than that of Portland cement, and further research is needed to investigate the shrinkage effects of SGM with gypsum and clinker, as well as the measures to mitigate shrinkage in alkali-activated systems.

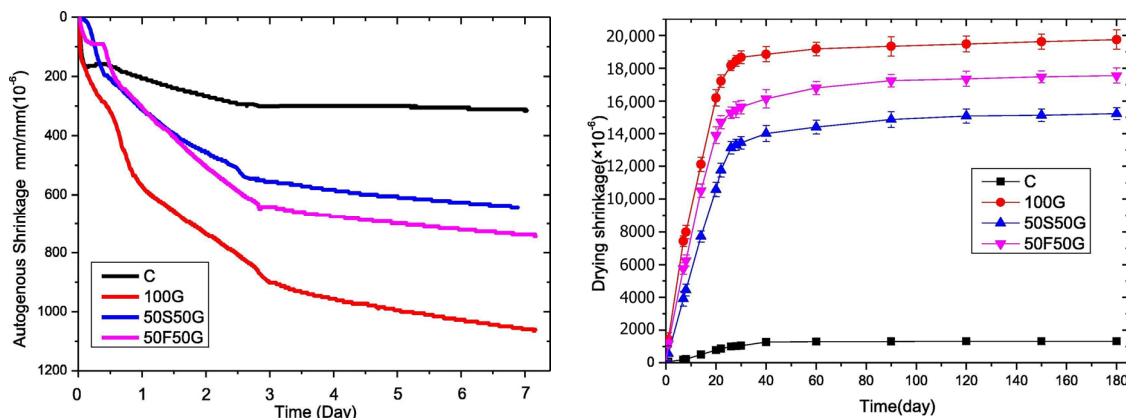


Figure 11. Autogenous shrinkage and drying shrinkage of cementitious materials [47].

5. Conclusions and Outlook

While steel slag and GBFS can exhibit some degree of synergistic hydration in water, the slow pozzolanic reaction of GBFS is attributed to the weak alkalinity generated by steel slag. To enhance the hydration rate, shorten the setting time, and improve the early strength, the addition of gypsum-based materials (such as natural gypsum and by-product gypsum), cement clinker, or alkaline activators (such as sodium silicate, $\text{Ca}(\text{OH})_2$, NaOH , Na_2CO_3 , etc.) can effectively optimize the SGM. Alkaline activators and clinker promote the hydration of steel slag and GBFS by increasing the alkalinity of the reaction system. In the case of SGM with gypsum, there is a clear ternary synergistic effect, leading to the formation of a dense matrix with Aft and C-S-H gel as the main reaction products. Despite the attention given to the hydration and hardening mechanisms, as well as the performance improvement mechanisms of SGM, there are still some unresolved issues:

- (1) A common issue with SGM is that as the steel slag content increases, the setting time lengthens and mechanical properties at an early age decrease. Given the high utilization rate and cost of GBFS in the market, as well as the low utilization rate and cost of steel slag, further research is needed to maximize the utilization of steel slag, reduce raw material costs, and ensure critical early-age performance.
- (2) There is limited research on the fresh properties of SGM. In practical engineering, fresh pastes need to meet certain requirements for setting time, workability, pumpability, and water retention. Therefore, identifying the factors and key indicators affecting fresh properties of SGM, as well as developing effective measures to improve them, requires further investigation.
- (3) SGM with gypsum holds promise as a solid waste system. However, there is still a lack of systematic research on the long-term mechanical properties, durability, and volume stability. In actual service environments, the secondary hydration of gypsum and the occurrence of “delayed Aft” may risk cracking in hardened pastes. Additionally, the presence of gypsum may lead to poor water resistance of the cementitious materials, necessitating further investigation.

Author Contributions: Conceptualization, methodology, writing—original draft, funding acquisition, J.S.; investigation, validation, formal analysis, resources, S.H.; methodology, investigation, Y.G.; investigation, formal analysis, X.C.; data curation, D.Z. All authors have read and agreed to the published version of the manuscript.

Funding: This research was funded by the Natural Science Fund of Shandong Province, ZR2023QE007, and the Open Project of Engineering Research Center of Concrete Technology under Marine Environment, TMduracon2022009.

Data Availability Statement: The raw data supporting the conclusions of this article will be made available by the authors on request.

Conflicts of Interest: Author Dongdong Zhang was employed by the company Jinan Rail Transit Group Co., Ltd. The remaining authors declare that the research was conducted in the absence of any commercial or financial relationships that could be construed as a potential conflict of interest.

References

1. Li, J.; Ni, W.; Wang, X.; Zhu, S.; Wei, X.; Jiang, F.; Zeng, H.; Hitch, M. Mechanical activation of medium basicity steel slag under dry condition for carbonation curing. *J. Build. Eng.* **2022**, *50*, 104123. [\[CrossRef\]](#)
2. Gao, W.; Zhou, W.; Lyu, X.; Liu, X.; Su, H.; Li, C.; Wang, H. Comprehensive utilization of steel slag: A review. *Powder Technol.* **2023**, *422*, 118449. [\[CrossRef\]](#)
3. Guo, J.L.; Bao, Y.P.; Wang, M. Steel slag in China, Treatment, recycling, and management. *Waste Manag.* **2018**, *78*, 318–330. [\[CrossRef\]](#) [\[PubMed\]](#)
4. Yang, M.Q.; Yang, J.Y. Vanadium extraction from steel slag: Generation, recycling and management. *Environ. Pollut.* **2024**, *343*, 123126. [\[CrossRef\]](#)
5. Aliyah, F.; Kambali, I.; Setiawan, A.F.; Radzi, Y.M.; Rahman, A.A. Utilization of steel slag from industrial waste for ionizing radiation shielding concrete: A systematic review. *Constr. Build. Mater.* **2023**, *382*, 131360. [\[CrossRef\]](#)
6. Kurniati, E.O.; Pederson, F.; Kim, H.-J. Application of steel slags, ferronickel slags, and copper mining waste as construction materials: A review. *Resour. Conserv. Recycl.* **2023**, *198*, 107175. [\[CrossRef\]](#)
7. Shu, K.; Sasaki, K. Occurrence of steel converter slag and its high value-added conversion for environmental restoration in China: A review. *J. Clean. Prod.* **2022**, *373*, 133876. [\[CrossRef\]](#)
8. O'Connor, J.; Nguyen, T.B.T.; Honeyands, T.; Monaghan, B.; O'Dea, D.; Rinklebe, J.; Vinu, A.; Hoang, S.A.; Singh, G.; Kirkham, M.B.; et al. Production, characterisation, utilisation, and beneficial soil application of steel slag: A review. *J. Hazard Mater.* **2021**, *419*, 126478. [\[CrossRef\]](#) [\[PubMed\]](#)
9. Tang, S.W.; Cai, R.J.; He, Z.; Cai, X.H.; Shao, H.Y.; Li, Z.J.; Yang, H.M.; Chen, E. Continuous microstructural correlation of slag/superplasticizer cement pastes by heat and impedance methods via fractal analysis. *Fractals* **2017**, *25*, 1740003. [\[CrossRef\]](#)
10. Zhuang, S.Y.; Wang, Q. Inhibition mechanisms of steel slag on the early-age hydration of cement. *Cem. Concr. Res.* **2021**, *140*, 106283. [\[CrossRef\]](#)
11. Yang, H.M.; Zhang, S.M.; Wang, L.; Chen, P.; Shao, D.K.; Tang, S.W.; Li, J.Z. High-ferrite Portland cement with slag: Hydration, microstructure, and resistance to sulfate attack at elevated temperature. *Cem. Concr. Comp.* **2022**, *130*, 104560–104576. [\[CrossRef\]](#)
12. Luo, T.; Wang, X.; Zhuang, S. Value-added utilization of steel slag as a hydration heat controlling material to prepare sustainable and green mass concrete. *Case Stud. Constr. Mater.* **2023**, *19*, e02619. [\[CrossRef\]](#)
13. Zhuang, S.Y.; Wang, Q.; Luo, T. Effect of C12A7 in steel slag on the early-age hydration of cement. *Cem. Concr. Res.* **2022**, *162*, 107010. [\[CrossRef\]](#)
14. Wang, Q.; Yan, P.Y. Hydration properties of basic oxygen furnace steel slag. *Constr. Build. Mater.* **2010**, *24*, 1134–1140. [\[CrossRef\]](#)
15. Sun, J.W.; Hou, S.Y.; Guo, Y.H. Effects of high-temperature curing on hydration and microstructure of alkali-activated typical steel slag cementitious material. *Dev. Built Environ.* **2024**, *17*, 100314. [\[CrossRef\]](#)
16. Li, Y.; Wu, B.H.; Ni, W.; Mu, X.L. Synergies in early hydration reaction of slag-steel slag-gypsum system. *J. Northeast. Univ.* **2020**, *41*, 581–586.
17. Cui, X.W.; Ni, W.; Reng, C. Chemical activation of cementitious materials with all solid waste based of steel slag and blast furnace slag. *Chin. J. Mater. Res.* **2017**, *9*, 687–694.
18. Wang, Q.; Yan, P.Y.; Feng, J.W. A discussion on improving hydration activity of steel slag by altering its mineral compositions. *J. Hazard. Mater.* **2011**, *186*, 1070–1075. [\[CrossRef\]](#) [\[PubMed\]](#)
19. Guo, X.L.; Shi, H.S. Effects of steel slag admixture with GGBFS on performances of cement paste and mortar. *Adv. Cem. Res.* **2015**, *26*, 93–100. [\[CrossRef\]](#)
20. Wang, Q.; Yan, P.Y.; Mi, G.D. Effect of blended steel slag-GBFS mineral admixture on hydration and strength of cement. *Constr. Build. Mater.* **2012**, *35*, 8–14. [\[CrossRef\]](#)
21. Singh, S.; Tripathy, D.; Ranjith, P. Performance evaluation of cement stabilized fly ash-GBFS mixes as a highway construction material. *Waste Manag.* **2008**, *28*, 1331–1337. [\[CrossRef\]](#)
22. Chen, P.; Ma, B.; Tan, H.; Wu, L.; Zheng, Z.; He, X.; Li, H.; Jin, Z.; Li, M.; Lv, Z. Improving the mechanical property and water resistance of β -hemihydrate phosphogypsum by incorporating ground blast-furnace slag and steel slag. *Constr. Build. Mater.* **2022**, *344*, 128265. [\[CrossRef\]](#)
23. Zeng, Q.; Liu, X.; Zhang, Z.; Xu, C.C. Synergistic utilization of blast furnace slag with other industrial solid wastes in cement and concrete industry, Synergistic mechanisms, applications, and challenges. *Green Energy Resour.* **2023**, *1*, 100012. [\[CrossRef\]](#)
24. Zhang, M.; Li, K.; Ni, W.; Zhang, S.; Liu, Z.; Wang, K.; Wei, X.; Yu, Y. Preparation of mine backfilling from steel slag-based non-clinker combined with ultra-fine tailing. *Constr. Build. Mater.* **2022**, *320*, 126248. [\[CrossRef\]](#)
25. Wang, Q.; Miao, M.; Feng, J.; Yan, P. The influence of high-temperature curing on the hydration characteristics of a cement-GGBS binder. *Adv. Cem. Res.* **2012**, *24*, 33–40. [\[CrossRef\]](#)

26. Xiao, B.; Wen, Z.; Miao, S.; Gao, Q. Utilization of steel slag for cemented tailings backfill: Hydration, strength, pore structure, and cost analysis. *Case Stud. Constr. Mater.* **2021**, *15*, e00621. [[CrossRef](#)]
27. Huang, X.; Wang, Z.; Liu, Y.; Hu, W.; Ni, W. On the use of blast furnace slag and steel slag in the preparation of green artificial reef concrete. *Constr. Build. Mater.* **2016**, *112*, 241–246. [[CrossRef](#)]
28. Wang, Q.; Yang, J.W.; Yan, P.Y. Cementitious properties of super-fine steel slag. *Powder Technol.* **2013**, *245*, 35–39. [[CrossRef](#)]
29. Zhou, Y.; Li, W.; Peng, Y.; Tang, S.; Wang, L.; Shi, Y.; Li, Y.; Wang, Y.; Geng, Z.; Wu, K. Hydration and fractal analysis on Low-heat Portland cement pastes by thermodynamic-based methods. *Fractal Fract.* **2023**, *7*, 606. [[CrossRef](#)]
30. Hamdan, A.; Song, H.; Yao, Z.; Alnahhal, M.F.; Kim, T.; Hajimohammadi, A. Modifications to reaction mechanisms, phase assemblages and mechanical properties of alkali-activated slags induced by gypsum addition. *Cem. Concr. Res.* **2023**, *174*, 107311. [[CrossRef](#)]
31. Li, Z.; Lu, T.; Liang, X.; Dong, H.; Ye, G. Mechanisms of autogenous shrinkage of alkali-activated slag and fly ash pastes. *Cem. Concr. Res.* **2020**, *135*, 106107. [[CrossRef](#)]
32. Fu, Q.; Bu, M.; Zhang, Z.; Xu, W.; Yuan, Q.; Niu, D. Hydration characteristics and microstructure of alkali-activated slag concrete: A review. *Engineering* **2023**, *20*, 162–179. [[CrossRef](#)]
33. Lee, K.M.; Park, P.J. Estimation of the environmental credit for the recycling of granulated blast furnace slag based on LCA. *Resour. Conserv. Recycl.* **2005**, *44*, 139–151. [[CrossRef](#)]
34. Zhao, J.; Li, Z.; Wang, D.; Yan, P.; Luo, L.; Zhang, H.; Zhang, H.; Gu, X. Hydration superposition effect and mechanism of steel slag powder and granulated blast furnace slag powder. *Constr. Build. Mater.* **2023**, *336*, 130101. [[CrossRef](#)]
35. Geng, Z.; Tang, S.; Wang, Y.; He, Z.; Wu, K. The stress relaxation properties of calcium silicate hydrate: A molecular dynamics study. *J. Zhejiang Univ.-Sci. A* **2023**, 1–22. [[CrossRef](#)]
36. Liao, Y.; Wang, S.; Wang, K.; Al Qunaynah, S.; Wan, S.; Yuan, Z.; Xu, P.; Tang, S. A study on the hydration of calcium aluminate cement pastes containing silica fume using non-contact electrical resistivity measurement. *J. Mater. Res. Technol.* **2023**, *24*, 8135–8149. [[CrossRef](#)]
37. Wang, L.; Guo, F.; Lin, Y.; Yang, H.; Tang, S.W. Comparison between the effects of phosphorous slag and fly ash on the C-S-H structure, long-term hydration heat and volume deformation of cement-based materials. *Constr. Build. Mater.* **2020**, *250*, 118807. [[CrossRef](#)]
38. Wang, L.; Jin, M.; Zhou, S.; Tang, S.; Lu, X. Investigation of microstructure of C-S-H and micro-mechanics of cement pastes under NH₄NO₃ dissolution by ²⁹Si MAS NMR and microhardness. *Measurement* **2021**, *185*, 110019. [[CrossRef](#)]
39. Wang, L.; Zhou, S.; Shi, Y.; Huang, Y.; Zhao, F.; Huo, T.; Tang, S. The influence of fly ash dosages on the permeability, pore structure and fractal features of face slab concrete. *Fractal Fract.* **2022**, *6*, 476. [[CrossRef](#)]
40. Wang, L.; Huang, Y.; Zhao, F.; Huo, T.; Chen, E.; Tang, S. Comparison between the influence of finely ground phosphorous slag and fly ash on frost resistance, pore structures and fractal features of hydraulic concrete. *Fractal Fract.* **2022**, *6*, 598. [[CrossRef](#)]
41. Tsai, C.J.; Huang, R.; Lin, W.T.; Chiang, H.W. Using GGBOS as the alkali activators in GGBS and GGBOS blended cements. *Constr. Build. Mater.* **2014**, *70*, 501–507. [[CrossRef](#)]
42. Meshram, S.; Raut, S.P.; Ansari, K.; Madurwar, M.; Daniyal, M.; Khan, M.A.; Katare, V.; Khan, A.H.; Khan, N.A.; Hasan, M.A. Waste slags as sustainable construction materials, a compressive review on physico mechanical properties. *J. Mate. Res. Technol.* **2023**, *23*, 5821–5845. [[CrossRef](#)]
43. Zhao, J. Grinding and Hydration Characteristics of Steel Slag and Composition and Properties of Composite Cementitious Materials Containing Steel. Ph.D. Thesis, China University of Mining and Technology, Beijing, China, 2015.
44. Xiong, X.; Yang, Z.; Yan, X.; Zhang, Y.; Dong, S.; Li, K.; Briseghella, B.; Marano, G.C. Mechanical properties and microstructure of engineered cementitious composites with high volume steel slag and GGBFS. *Constr. Build. Mater.* **2014**, *70*, 501–507. [[CrossRef](#)]
45. Ghorbani, S.; Stefanini, L.; Sun, Y.; Walkley, B.; Provis, J.L.; De Schutter, G.; Matthys, S. Characterisation of alkali-activated stainless steel slag and blast-furnace slag cements. *Cem. Concr. Compos.* **2023**, *143*, 105230. [[CrossRef](#)]
46. Siddique, R.; Bennacer, R. Use of iron and steel industry by-product (GGBS) in cement paste and mortar. *Resour. Conserv. Recycl.* **2012**, *69*, 29–34. [[CrossRef](#)]
47. You, N.; Li, B.; Cao, R.; Shi, J.; Chen, C.; Zhang, Y. The influence of steel slag and ferronickel slag on the properties of alkali-activated slag mortar. *Constr. Build. Mater.* **2019**, *227*, 116614. [[CrossRef](#)]
48. Li, J.S.; Li, J.M.; Ge, X.X. Preparation and characterization of early strengthened of binding materials steel slag and blast furnace slag. *J. Anhui Univ. Technol. (Nat. Sci.)* **2020**, *37*, 321–326.
49. Zhou, Y.Q.; Sun, J.; Liao, Y.W. Influence of ground granulated blast furnace slag on the early hydration and microstructure of alkali-activated converter steel slag binder. *J. Therm. Anal. Calorim.* **2020**, *182*, 243–252. [[CrossRef](#)]
50. Sun, J.W.; Chen, Z.H. Effect of silicate modulus of water glass on the hydration of alkali-activated converter steel slag. *J. Therm. Anal. Calorim.* **2019**, *138*, 47–56. [[CrossRef](#)]
51. Atiş, C.D.; Bilim, C.; Çelik, Ö.; Karahan, O. Influence of activator on the strength and drying shrinkage of alkali-activated slag mortar. *Constr. Build. Mater.* **2009**, *23*, 548–555. [[CrossRef](#)]
52. Luukkonen, T.; Sreenivasan, H.; Abdollahnejad, Z.; Yliniemi, J.; Kantola, A.; Telkki, V.V.; Kinnunen, P.; Illikainen, M. Influence of sodium silicate powder silica modulus for mechanical and chemical properties of dry-mix alkali-activated slag mortar. *Constr. Build. Mater.* **2020**, *233*, 117354. [[CrossRef](#)]

53. Liu, Z.; Ni, W.; Li, Y.; Ba, H.; Li, N.; Ju, Y.; Zhao, B.; Jia, G.; Hu, W. The mechanism of hydration reaction of granulated blast furnace slag-steel slag-refining slag-desulfurization gypsum-based clinker-free cementitious materials. *J. Build. Eng.* **2021**, *40*, 103289. [[CrossRef](#)]
54. Li, Y.; Liang, W.; Ni, W.; Mu, X.; Li, Y.; Fan, K. Characteristics of hydration and hardening of steel slag mud-blast furnace slag-desulphurization gypsum system. *Bull. Chin. Ceram. Soc.* **2022**, *41*, 536–544.
55. Liao, Y.; Yao, J.; Deng, F.; Li, H.; Wang, K.; Tang, S. Hydration behavior and strength development of supersulfated cement prepared by calcined phosphogypsum and slaked lime. *J. Build. Eng.* **2023**, *80*, 108075. [[CrossRef](#)]
56. Xu, C.; Ni, W.; Li, K.; Zhang, S.; Xu, D. Activation mechanisms of three types of industrial by-product gypsums on steel slag-granulated blast furnace slag-based binders. *Constr. Build. Mater.* **2021**, *288*, 123111. [[CrossRef](#)]
57. Zhao, J.H.; Wang, D.M.; Yan, P.Y. Design and experimental study of a ternary blended cement containing high volume steel slag and blast-furnace slag based on Fuller distribution model. *Constr. Build. Mater.* **2017**, *140*, 248–256. [[CrossRef](#)]
58. Li, Y.; Zhang, H.; Huang, M.; Yin, H.; Jiang, K.; Xiao, K.; Tang, S. Influence of different alkali sulfates on the shrinkage, hydration, pore structure, fractal dimension and microstructure of low-heat Portland cement, medium-heat Portland cement and ordinary Portland cement. *Fractal Fract.* **2021**, *5*, 79. [[CrossRef](#)]
59. Feng, J.J.; Sun, J.W. A comparison of the 10-year properties of converter steel slag activated by high temperature and an alkaline activator. *Constr. Build. Mater.* **2020**, *234*, 116948. [[CrossRef](#)]
60. Maria, C.; Willian, A.; Isabel, S. Microstructural and mechanical properties of alkali activated colombian raw materials. *Materials* **2016**, *9*, 158.
61. Sun, J.; Zhang, Z.; Zhuang, S.; He, W. Hydration properties and microstructure characteristics of alkali-activated steel slag. *Constr. Build. Mater.* **2020**, *241*, 118141. [[CrossRef](#)]
62. Cao, R.; Li, B.; You, N.; Zhang, Y.; Zhang, Z. Properties of alkali-activated ground granulated blast furnace slag blended with ferronickel slag. *Constr. Build. Mater.* **2018**, *192*, 123–132. [[CrossRef](#)]
63. Zhang, G.Q.; Wu, P.C.; Gao, S.J. Properties and microstructure of low-carbon whole-tailings cemented paste backfill material containing steel slag, granulated blast furnace slag and flue gas desulphurization gypsum. *Acta Microsc.* **2019**, *28*, 770–780.
64. Brakat, A.; Zhang, Y. Shrinkage mitigation of alkali activated slag with natural cellulose fibers. *Adv. Cem. Res.* **2017**, *31*, 47–57. [[CrossRef](#)]
65. Furlani, E.; Maschio, S.; Magnan, M.; Aneggi, E.; Andreatta, F.; Lekka, M.; Lanzutti, A.; Fedrizzi, L. Synthesis and characterization of geopolymers containing blends of unprocessed steel slag and metakaolin: The role of slag particle size. *Ceram. Int.* **2018**, *44*, 5226–5232. [[CrossRef](#)]
66. Hu, S.G.; He, Y.J.; Lu, L.N.; Ding, Q.J. Effect of fine steel slag powder on the early hydration process of Portland cement. *J. Wuhan Univ. Technol. (Mater. Sci. Ed.)* **2006**, *21*, 147–149.
67. Altun, I.A.; Yilmaz, İ. Study on steel furnace slags with high MgO as additive in Portland cement. *Cem. Concr. Res.* **2002**, *32*, 1247–1249. [[CrossRef](#)]
68. Liu, K.S.; Zhang, Z.Q.; Sun, J.W. Advances in understanding the alkali-activated metallurgical slag. *Adv. Civ. Eng.* **2021**, *2021*, 8795588. [[CrossRef](#)]
69. Xu, C.; Ni, W.; Li, K.; Zhang, S.; Li, Y.; Xu, D. Hydration mechanism and orthogonal optimisation of mix proportion for steel slag-slag-based clinker-free prefabricated concrete. *Constr. Build. Mater.* **2019**, *228*, 117036. [[CrossRef](#)]
70. Xiao, B. Steel Slag Binder and Its Application in the Cemented Tailings Backfill. Ph.D. Thesis, University of Science and Technology, Beijing, China, 2020.
71. Adesanya, E.; Ohenoja, K.; Di Maria, A.; Kinnunen, P.; Illikainen, M. Alternative alkali-activator from steel-making waste for one-part alkali-activated slag. *J. Clean. Prod.* **2020**, *274*, 123020. [[CrossRef](#)]
72. Han, F.H.; Yan, P.Y. Hydration characteristics of slag-blended cement at different temperatures. *J. Sustain. Cem.-Based Mater.* **2015**, *4*, 34–43. [[CrossRef](#)]
73. Clark, B.A.; Brown, P.W. Formation of calcium sulfoaluminate hydrate compounds. *Cem. Concr. Res.* **2000**, *30*, 233–240. [[CrossRef](#)]
74. Gruszczinski, E.; Brown, P.W.; Both, J.V., Jr. The formation of ettringite at elevated temperature. *Cem. Concr. Res.* **1993**, *23*, 981–987. [[CrossRef](#)]
75. Wang, M.; Qian, B.; Jiang, J.; Liu, H.; Cai, Q.; Ma, B.; Hu, Y.; Wang, L. The reaction between Ca²⁺ from steel slag and granulated blast-furnace slag system, a unique perspective. *Chem. Pap.* **2020**, *74*, 4401–4410. [[CrossRef](#)]
76. Xiang, X.D.; Xi, J.C.; Li, C.H.; Jiang, X.W. Preparation and application of the cement-free steel slag cementitious material. *Constr. Build. Mater.* **2016**, *114*, 874–879. [[CrossRef](#)]
77. Li, Q.; Zhao, F.Q.; Li, H.; Zhang, R.; Liu, L. Durability of slag and steel slag-based cementitious materials. *China Concr. Cem. Prod.* **2011**, *1*, 23–27.
78. Wang, X.; Ni, W.; Li, J.; Zhang, S.; Hitch, M.; Pascual, R. Carbonation of steel slag and gypsum for building materials and associated reaction mechanisms. *Cem. Concr. Res.* **2019**, *125*, 105893. [[CrossRef](#)]
79. You, N.Q.; Shi, J.J.; Zhang, Y.M. Corrosion behaviour of low-carbon steel reinforcement in alkali-activated slag-steel slag and Portland cement-based mortars under simulated marine environment. *Corros. Sci.* **2020**, *175*, 108874. [[CrossRef](#)]
80. Shi, C.J.; Qu, B.; Provis, J.L. Recent progress in low-carbon binders. *Cem. Concr. Res.* **2019**, *122*, 227–250. [[CrossRef](#)]
81. Zhang, B.; Zhu, H.; Feng, P.; Zhang, P. A review on shrinkage-reducing methods and mechanisms of alkali-activated/geopolymer systems: Effects of chemical additives. *J. Build. Eng.* **2022**, *49*, 104056. [[CrossRef](#)]

82. Liu, S.H.; Li, Q.L.; Han, W.W. Effect of various alkalis on hydration properties of alkali-activated slag cements. *J. Therm. Anal. Calorim.* **2018**, *131*, 3093–3104. [[CrossRef](#)]
83. Hou, D.H.; Li, T.; Wang, P. Molecular dynamics study on the structure and dynamics of NaCl solution transport in the nanometer channel of CASH gel. *ACS Sustain. Chem. Eng.* **2018**, *7*, 9498–9509. [[CrossRef](#)]
84. Sun, X.; Peng, X.; Zhang, G.; Wang, S.; Zeng, L. Effect of steel slag content on properties of alkali-activated steel slag and slag based grouting material. *New Build. Mater.* **2017**, *44*, 10–13.
85. Darko, K.; Branislav, Z. Effects of dosage and modulus of water glass on early hydration of alkali-slag cements. *Cem. Concr. Res.* **2002**, *32*, 1181–1188.
86. Bernal, S.A.; de Gutierrez, R.M.; Provis, J.L.; Rose, V. Effect of silicate modulus and metakaolin incorporation on the carbonation of alkali silicate-activated slags. *Cem. Concr. Res.* **2010**, *40*, 898–907. [[CrossRef](#)]

Disclaimer/Publisher’s Note: The statements, opinions and data contained in all publications are solely those of the individual author(s) and contributor(s) and not of MDPI and/or the editor(s). MDPI and/or the editor(s) disclaim responsibility for any injury to people or property resulting from any ideas, methods, instructions or products referred to in the content.